



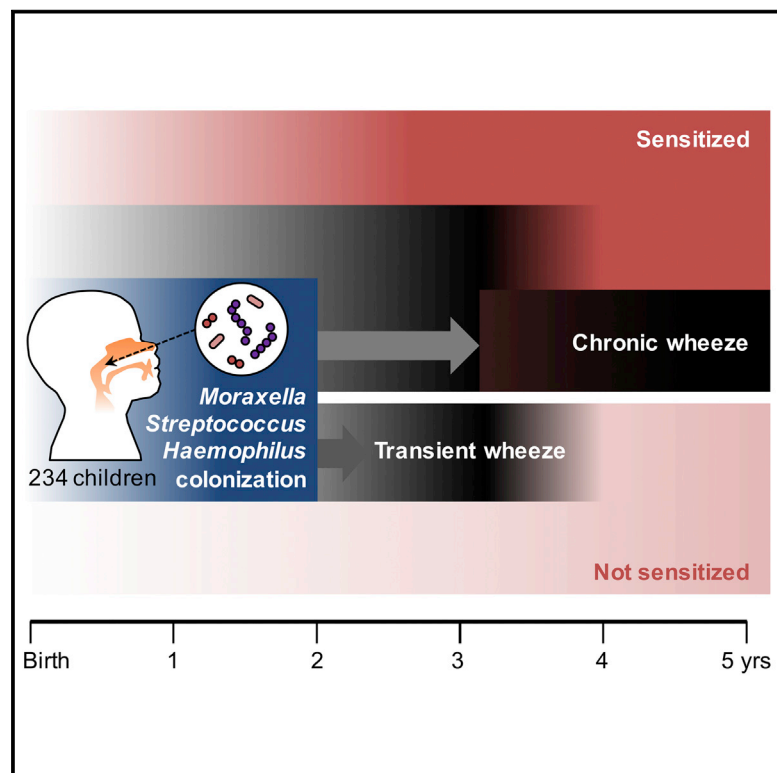
Since January 2020 Elsevier has created a COVID-19 resource centre with free information in English and Mandarin on the novel coronavirus COVID-19. The COVID-19 resource centre is hosted on Elsevier Connect, the company's public news and information website.

Elsevier hereby grants permission to make all its COVID-19-related research that is available on the COVID-19 resource centre - including this research content - immediately available in PubMed Central and other publicly funded repositories, such as the WHO COVID database with rights for unrestricted research re-use and analyses in any form or by any means with acknowledgement of the original source. These permissions are granted for free by Elsevier for as long as the COVID-19 resource centre remains active.

Cell Host & Microbe

Airway Microbiota Dynamics Uncover a Critical Window for Interplay of Pathogenic Bacteria and Allergy in Childhood Respiratory Disease

Graphical Abstract



Authors

Shu Mei Teo, Howard H.F. Tang, Danny Mok, ..., Patrick G. Holt, Kathryn E. Holt, Michael Inouye

Correspondence

kholt@unimelb.edu.au (K.E.H.),
mi336@medschl.cam.ac.uk (M.I.)

In Brief

Teo et al. characterize nasopharyngeal microbiota (NPM) in 244 children from birth to age 5 years during periods of illness and health. NPM colonization with illness-associated bacteria may promote acute respiratory illness independent of viral infection, and is associated with chronic or transient wheeze in allergic-sensitized or non-sensitized children, respectively.

Highlights

- Six genera dominate airway microbiota from birth to 2 years, but diversifies thereafter
- Acute respiratory illness associates with pathogenic bacteria in the airway microbiota
- Pathogenic airway bacteria may precede viral incursions and acute respiratory illness
- Colonization with pathogens predicts chronic wheeze in allergic-sensitized children



Airway Microbiota Dynamics Uncover a Critical Window for Interplay of Pathogenic Bacteria and Allergy in Childhood Respiratory Disease

Shu Mei Teo,^{1,2,3} Howard H.F. Tang,^{1,2,4} Danny Mok,⁵ Louise M. Judd,³ Stephen C. Watts,³ Kym Pham,⁶ Barbara J. Holt,⁵ Merci Kusel,⁵ Michael Serralha,⁵ Niamh Troy,⁵ Yury A. Bochkov,⁷ Kristine Grindle,⁷ Robert F. Lemanske, Jr.,⁷ Sebastian L. Johnston,⁸ James E. Gern,⁷ Peter D. Sly,⁹ Patrick G. Holt,^{5,9} Kathryn E. Holt,^{3,5,10,12,*} and Michael Inouye^{1,2,4,5,6,11,12,13,*}

¹Cambridge Baker Systems Genomics Initiative, Baker Heart and Diabetes Institute, Melbourne, VIC 3004, Australia

²Cambridge Baker Systems Genomics Initiative, Department of Public Health and Primary Care, University of Cambridge, Cambridge CB1 8RN, UK

³Department of Biochemistry and Molecular Biology, Bio21 Molecular Science and Biotechnology Institute, University of Melbourne, Parkville, VIC 3010, Australia

⁴School of BioSciences, The University of Melbourne, Parkville, VIC 3010, Australia

⁵Telethon Kids Institute, The University of Western Australia, West Perth, WA, Australia

⁶Department of Clinical Pathology, The University of Melbourne, Parkville, VIC 3010, Australia

⁷University of Wisconsin School of Medicine and Public Health, Madison, WI 53705, USA

⁸Airway Disease Infection Section and MRC & Asthma UK Centre in Allergic Mechanisms of Asthma, National Heart and Lung Institute, Imperial College London, Norfolk Place, London W2 1PG, UK

⁹Child Health Research Centre, The University of Queensland, Brisbane 4101, Australia

¹⁰The London School of Hygiene and Tropical Medicine, London WC1E 7HT, UK

¹¹The Alan Turing Institute, London, UK

¹²These authors contributed equally

¹³Lead Contact

*Correspondence: kholt@unimelb.edu.au (K.E.H.), mi336@medschl.cam.ac.uk (M.I.)

<https://doi.org/10.1016/j.chom.2018.08.005>

SUMMARY

Repeated cycles of infection-associated lower airway inflammation drive the pathogenesis of persistent wheezing disease in children. In this study, the occurrence of acute respiratory tract illnesses (ARIs) and the nasopharyngeal microbiome (NPM) were characterized in 244 infants through their first five years of life. Through this analysis, we demonstrate that >80% of infectious events involve viral pathogens, but are accompanied by a shift in the NPM toward dominance by a small range of pathogenic bacterial genera. Unexpectedly, this change frequently precedes the detection of viral pathogens and acute symptoms. Colonization of illness-associated bacteria coupled with early allergic sensitization is associated with persistent wheeze in school-aged children, which is the hallmark of the asthma phenotype. In contrast, these bacterial genera are associated with “transient wheeze” that resolves after age 3 years in non-sensitized children. Thus, to complement early allergic sensitization, monitoring NPM composition may enable early detection and intervention in high-risk children.

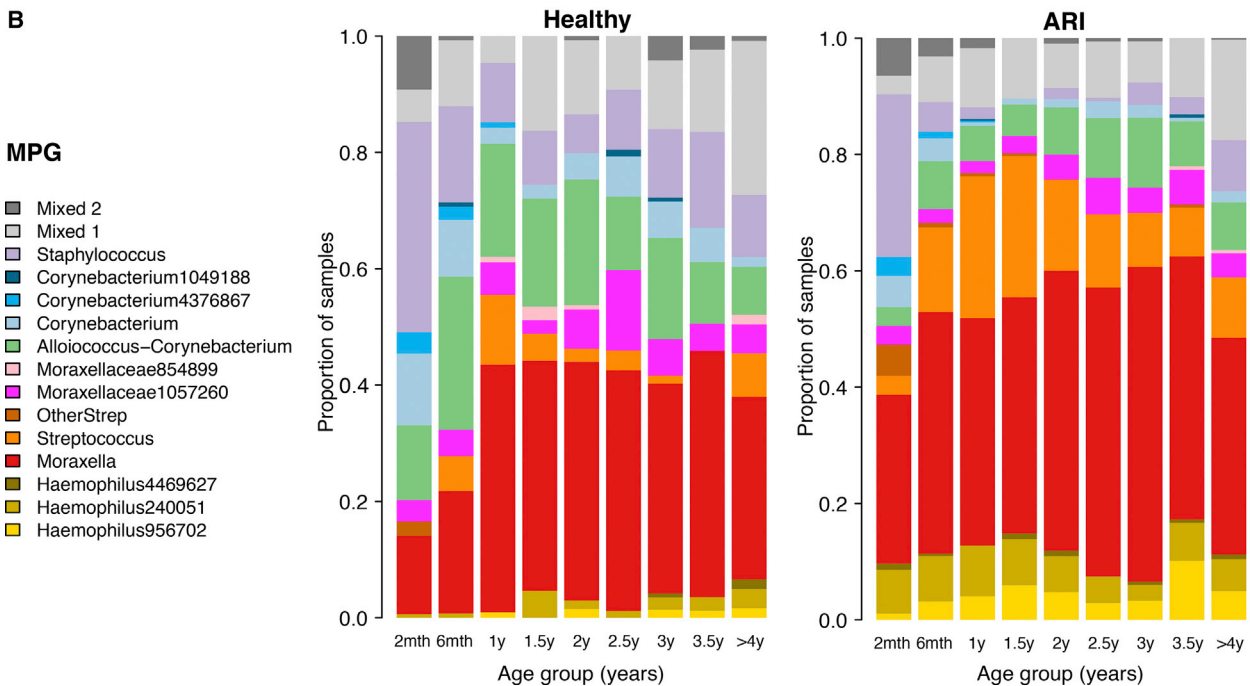
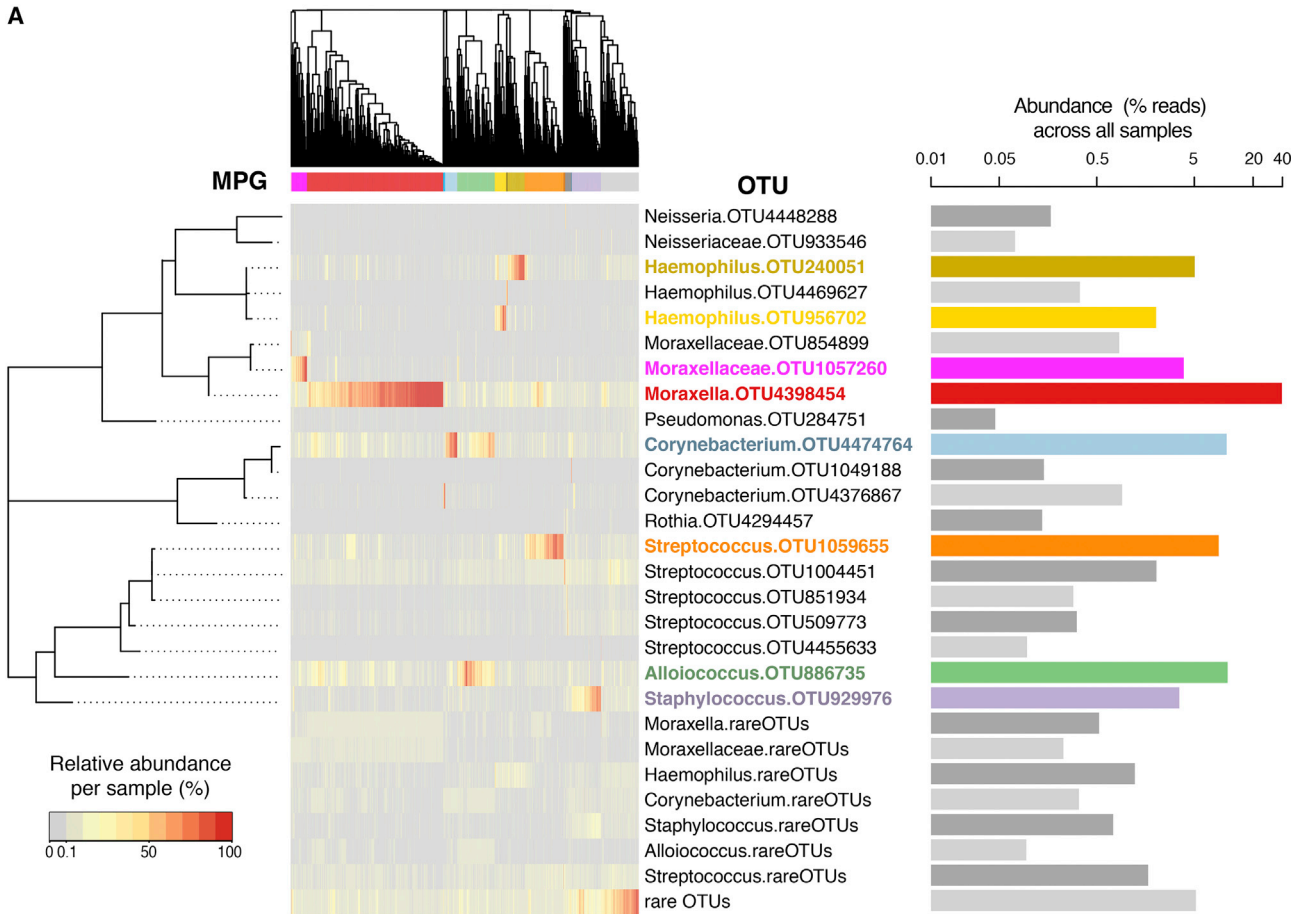
INTRODUCTION

Despite advances in modern medicine, acute respiratory tract illnesses (ARIs) continue to be a global health concern. They

are a major cause of morbidity and mortality, especially in infants and young children whose immune systems have not yet matured (Ferkol and Schraufnagel, 2014; Zar and Ferkol, 2014), and are the most common reason for antibiotic use in children (Australian Commission on Safety and Quality in Health Care, 2017). The upper airway is a reservoir for microbial communities including viruses, bacteria, and fungi, and these have implications for respiratory health and disease. However, current research into the etiology of ARIs focuses primarily on viruses, most notably respiratory syncytial virus (RSV) and human rhinoviruses (RV). The bacterial microbiome is increasingly recognized as playing an important role in the susceptibility and severity of ARIs, as well as non-communicable respiratory diseases such as asthma (de Steenhuijsen Piters et al., 2015; Durack et al., 2016; Man et al., 2017; Vissers et al., 2014). Infancy is a critical time when microbial colonization may influence an individual’s future respiratory health or disease; indeed, epidemiological data show that repeated ARIs during early childhood are a major risk factor for wheeze and asthma that persist into adulthood (Holt and Sly, 2012).

In recent years, we and others have described the nasopharyngeal microbiome (NPM) in early life (from birth to 1 or 2 years of age) (Biesbroek et al., 2014; Bisgaard et al., 2007; Bogaert et al., 2011; Bosch et al., 2017; Teo et al., 2015; Tsai et al., 2015). These independent studies in different human populations have reported strikingly similar findings. Firstly, the NPM appears to be simple in structure, with distinct profiles dominated by a single bacterial operational taxonomic unit (OTU) or genus. A *Staphylococcus*-dominated profile can be observed in early infancy (from 1 week) but its prevalence decreases





(legend on next page)

sharply over the first year, to be replaced by *Corynebacterium*-, *Alloiococcus* (*Dolosigranulum*)-, or *Moraxella*-dominated profiles, with transient incursions of *Streptococcus*- or *Haemophilus*-dominated profiles during ARIs. Secondly, NPM composition influences both microbiota stability and ARI risk and severity. One study of 60 infants from the Netherlands in the first two years of life reported a *Moraxella*-dominated or mixed *Corynebacterium*/*Dolosigranulum* profile at 1.5 months of age was associated with high NPM stability and low frequency of parent-reported ARIs in the subsequent period (Biesbroek et al., 2014). Our study of 234 infants from Australia in the first year of life also found that *Moraxella*-dominated and *Alloiococcus*-dominated profiles were more stable than others, but a *Moraxella*-dominated NPM at 2 months of age was associated with earlier onset of first ARI (Teo et al., 2015). There were also common environmental correlates of the NPM that differed slightly across studies but included mode of delivery, infant feeding, season, crowding or exposure to other children, recent antibiotic use, and prior infections. Many of these studies, however, were limited to samples collected either during illness or during periods of health, and none have yet elucidated the dynamics of the NPM over the entire pre-school period.

Understanding patterns of airway microbial colonization and its association with ARIs and subsequent wheeze phenotypes is an important step toward the potential manipulation of the microbiome in treating or preventing acute or chronic respiratory disease. In this study, we performed a comprehensive characterization of the largest longitudinal collection of nasopharyngeal samples reported to date: more than 3,000 samples from 244 children collected during periods of respiratory health and acute illness over the first five years of life, as part of the prospective Childhood Asthma Study (CAS) (Kusel et al., 2006, 2007, 2008, 2012; Teo et al., 2015). We have previously reported an association between viral-associated lower respiratory infections (LRIs) in infancy, especially those accompanied by fever, and the development of persistent wheeze and asthma in later childhood at 5 and 10 years of age in this cohort, particularly for infants who developed allergic sensitization by age 2 (Kusel et al., 2007, 2012). In addition, we recently reported patterns of bacterial colonization in samples collected during the first year of life, and found that specific NPM profiles were associated with ARI symptom severity, independent of the effect of common respiratory viruses (Teo et al., 2015). Here, we address several major research gaps: (1) we examine the relationships and longitudinal dynamics of NPM colonization within children, in health and during ARI episodes, across the first five years of life; (2) we investigate changes in the association of ARI symptoms with specific NPM taxa over the pre-school years; (3) we address whether the appearance of viral pathogens in the NPM is a harbinger of change in local bacterial populations, or vice versa;

and (4) we investigate the relationship between NPM colonization, early allergic sensitization, and future persistent wheeze at 5 years of age.

RESULTS

We characterized the bacterial microbiome of 3,014 nasopharyngeal samples from 244 infants in their first five years of life, using 16S rRNA V4 region amplicon sequencing (STAR Methods).

Composition of Upper Airway Microbiota in the First Five Years of Life

Across all samples, the dominant bacterial genera were *Moraxella* (40.1%), *Streptococcus* (13.3%), *Corynebacterium* (12.1%), *Alloiococcus* (11.1%), *Haemophilus* (8.6%), and *Staphylococcus* (4.2%). These made up 89% of all reads, consistent with previously reported results in this cohort for the first year of life (Teo et al., 2015) (Figures 1A and S1A). Each of the six major genera comprised multiple OTUs, although the majority were extremely rare. OTU distributions within *Moraxella*, *Alloiococcus*, and *Corynebacterium* were less diverse, with ≤ 5 OTUs making up $\geq 97\%$ of all reads from each respective genus at any time period (Figure S1B). OTU distributions within *Streptococcus*, *Haemophilus*, and *Staphylococcus* were more diverse, although still dominated by one or two OTUs (Figure S1B). The phylogenetic relationships between OTUs are indicated by the tree in Figure 1A, and details of their distribution and predicted species associations are discussed in Figure S2 and Table S1.

The distribution of the relative abundances of common OTUs across samples was highly structured (Figure 1A). We used hierarchical clustering to assign each sample to one of 15 microbiome profile groups (MPGs) (Figure 1). Most MPGs were dominated by one OTU, which was used to label each MPG (Figure 1 and Table S2). The exceptions were two “mixed” MPGs. “Mixed1” MPG contains samples ($n = 327$) in which the common OTUs were all at low abundance, and the vast majority of mixed1 samples (97%) were not dominated by any OTU; the rest were mostly ARI samples dominated by genera that likely represent known respiratory pathogens (*Mycoplasma*, *Bordetella*, *Neisseria*, *Pseudomonas*, *Prevotella*). “Mixed2” MPG ($n = 51$) represents a heterogeneous cluster with no distinct profile. The distribution of MPGs across ages is shown in Figure 1B.

Within-sample (alpha) diversity of the NPM increased with age in both healthy and ARI samples, with a noticeable increase after 2 years of age (generalized estimating equations linear regression of Shannon’s diversity index versus age, adjusted for symptom status and gender: $p = 1.1 \times 10^{-12}$ after 2 years; Figure 2A). The increasing diversity after 2 years of age was due to both increasing number and increasing equitability (evenness) of the

Figure 1. Definition and Distribution of Microbiome Profile Groups

(A) Heatmap shows relative abundances of 20 common operational taxonomic units (OTUs), aggregated values for other OTUs from the common genera, and aggregated values for all other rare OTUs within each sample. Tree to the left shows phylogenetic relationships between the sequenced V4 region of the 21 common OTU sequences. Dendrogram at the top indicates complete linkage clustering of Bray-Curtis distances between samples; colored bars indicate assignment to microbiome profile groups (MPGs) based on this clustering. Bar plot to the right shows the total abundance of each OTU or group of OTUs within the whole dataset; OTUs that dominate a common MPG are colored to match that MPG.

(B) Distribution of MPGs within each time period, shown separately for healthy and acute respiratory illness (ARI) samples. See also Figures S1 and S2; Table S2.

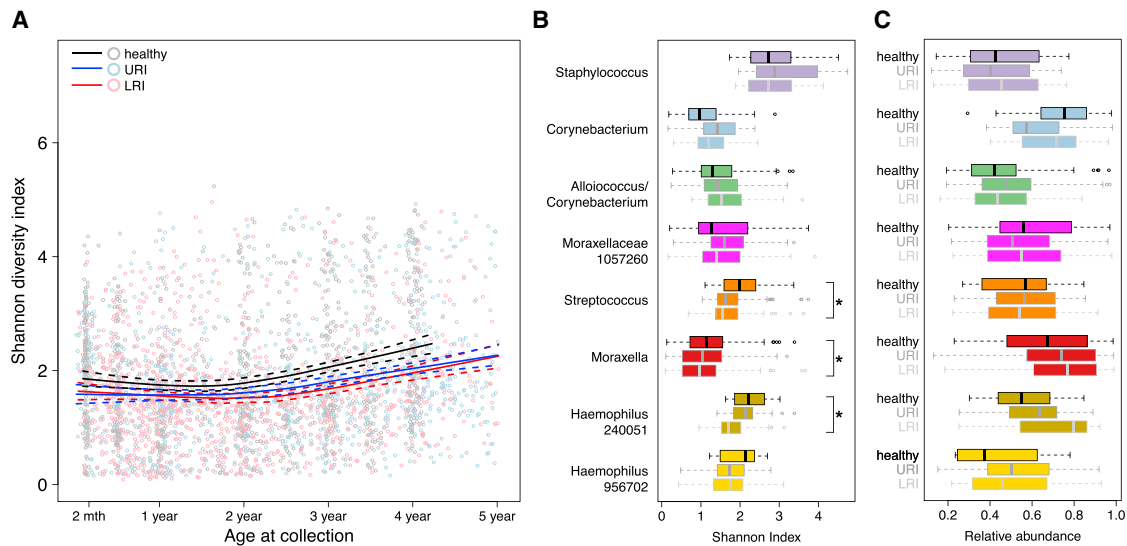


Figure 2. Within-Sample Diversity Is Associated with Age and Acute Respiratory Illness Symptoms

(A) Shannon diversity index (SDI) per sample over time, colored by symptom status as indicated (URI, upper respiratory illness; LRI, lower respiratory illness). Solid lines, loess smoothed curves; dashed lines, 95% confidence intervals.

(B) SDI distributions within common MPGs. Asterisk indicates FDR adjusted p value of <0.05 in GEE linear regression of SDI against healthy versus LRI, adjusted for age at collection (as in Table S3).

(C) Relative abundances of the dominant OTU within each MPG (as specified in Table S1).

See also Figure S3 and Table S3.

OTUs (Figures S3A and S3B), and this trend was observed within all MPGs (Figure S3C).

Upper Airway Bacteria and Respiratory Infection

Consistent with our previously reported observations from the first year of life (Teo et al., 2015), ARI was positively associated with MPGs dominated by *Haemophilus* (odds ratio [OR] 4.6, $p = 1.9 \times 10^{-12}$), *Streptococcus* (OR 3.9, $p = 1.7 \times 10^{-17}$), or *Moraxella* (OR 1.3, $p = 1.8 \times 10^{-4}$) (Table S2). Within these MPGs, the relative abundance of the dominant OTU increased and the alpha diversity decreased with symptom severity (comparing healthy, with upper respiratory illness [URI], with LRI; Figure 2B and Table S3). Thus overgrowth of these taxa accompanies spread of infection to the lower airways, although the direction of causation is not resolvable here.

At the OTU level, the relative abundances of 236 OTUs (present in $>10\%$ of samples) were significantly different between ARI and healthy samples (absolute difference >1.5 -fold and false discovery rate [FDR] adjusted p value <0.05). However, these associations were age dependent and appeared to shift following the increase in within-sample diversity observed from 2 years of age. Comparing the time periods before year 2 and on or after the second birthday, a total of 310 OTUs were found to be significantly associated with ARI in at least one interval (absolute difference >1.5 -fold and FDR adjusted p value <0.025 ; Figure S4A). The majority of *Moraxella*, *Haemophilus*, and *Streptococcus* OTUs were consistently positively associated with ARI in both time periods. *Staphylococcus*, *Corynebacterium*, and *Alloiooccus* OTUs were negatively associated with ARI in the first 2 years but these associations waned after 2 years, particularly for *Corynebacterium* and *Alloiooccus* (Figure S4A). Adjusting for

the most common ARI-associated OTU, *Moraxella* 4398454 (Figure S4B) resulted in little change to these associations, suggesting that *Moraxella* 4398454 and other OTUs contribute independently to ARI risk. Interestingly, we found two *Streptococcus* OTUs that were negatively associated with ARI (OTUs 4365744 and 509773, which show closest match to species *gordonii* and *thermophilus/salivarius/vestibularis*, respectively; Table S1 and Figure S2A). These were positively correlated with one other (SparCC correlation 0.09, $p = 0.001$), but negatively correlated with *Streptococcus* OTU 1059655 (SparCC correlation -0.09 and -0.1 , respectively; $p = 0.001$), which has closest match to *pneumoniae/pseudopneumoniae*. The set of five MPGs dominated by ARI-associated *Moraxella*, *Streptococcus*, or *Haemophilus* OTUs are collectively termed here “illness-associated MPGs” (Table S2). Among the rare OTUs, eight including from genera *Nitriliruptor* and *Bacillus* were consistently health associated and often co-occurred together (at median relative abundance 9%) in samples belonging to the *Staphylococcus* MPG, while a further eight OTUs including from genera *Porphyromonas*, *Candidatus*, *Aquiluna*, *Clavibacter*, *Mycobacterium*, *Granulicatella*, and *Fusobacterium* were consistently ARI associated but generally of low abundance across all MPGs (Figures S4C and S4D).

To more precisely estimate how these associations change with age, we performed time-varying analysis for eight characteristic OTUs using smoothing splines ANOVA (STAR Methods). The results showed that the strength of association of *Corynebacterium*, *Alloiooccus*, and *Staphylococcus* with healthy samples was greatest in the first 1–2 years; interestingly the association waned toward the null by 3 years of age for *Corynebacterium* and 4 years of age for *Staphylococcus*, but *Alloiooccus*

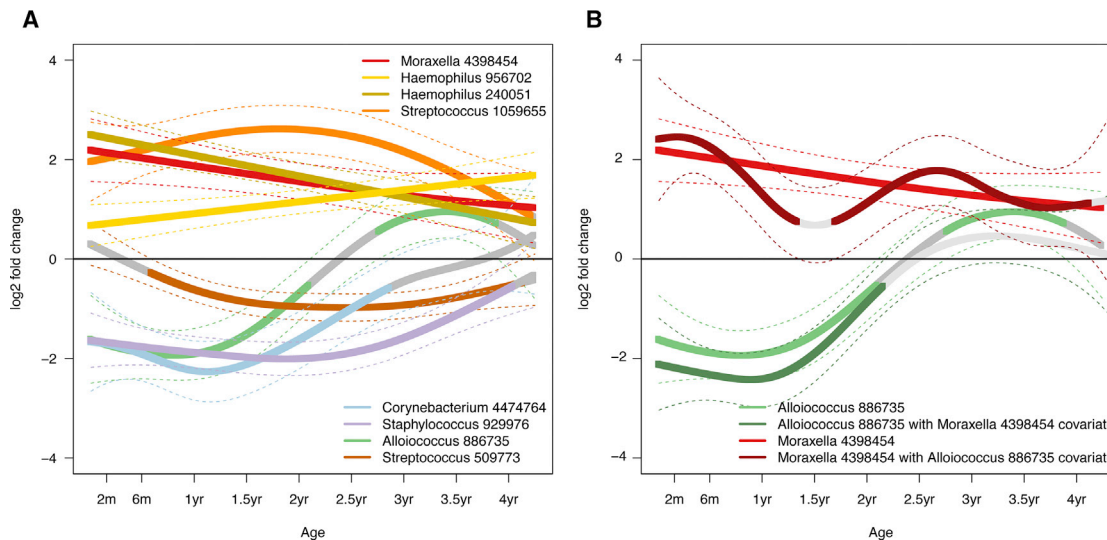


Figure 3. Time-Varying Associations of Bacterial Taxa with Acute Respiratory Illness Symptoms

(A) Log₂ fold change (solid lines) and 95% confidence intervals (dashed lines) comparing symptomatic versus healthy samples, estimated using smoothing splines ANOVA. Non-significant segments are colored gray.

(B) Same as (A) but including further adjustment for *Moraxella* OTU 4398454 abundance (dark-green curve) and vice versa (dark-red curve).

See also Figure S4.

changed direction and was significantly associated with ARI in the interval 2.8–3.9 years (mean difference 1.8-fold, $p = 0.01$) (Figure 3A). *Alloiooccus otitidis* in the ear canal has been implicated in otitis media (OM) (Harimaya et al., 2006; Tano et al., 2008), along with *Streptococcus pneumoniae* and *Haemophilus influenzae* (Ngo et al., 2016). In this cohort, 11% of ARI episodes co-occurred with OM. *Streptococcus* OTU 1059655 abundance in the NPM during ARI was positively associated with concurrent OM from 18 months (mean difference 2.4-fold, $p = 0.01$), but *Alloiooccus* and *Haemophilus* showed no significant associations with OM. The *Alloiooccus*-illness association is further addressed below.

Co-occurrence of Bacteria and Viruses in the Upper Airways and Their Association with Respiratory Illness

We calculated pairwise correlation networks between OTUs separately for samples collected before 2 years of age and on or after the second birthday; values for the eight most common OTUs are shown in Figure 4A. Illness-associated OTUs of *Moraxella*, *Haemophilus*, and *Streptococcus* formed a group that were all positively correlated with one another in both time periods, and negatively correlated with the health-associated *Streptococcus* OTU 509773 and *Staphylococcus* (Figure 4A). *Corynebacterium* and *Alloiooccus* were strongly correlated with one another in both periods (SparCC correlation = 0.68, $p = 0.001$). Surprisingly, the relationship between these OTUs and those in the illness-associated group (Figure 4A) was complex and changed over time, becoming significantly more positively correlated with age (Figure 4B). *Corynebacterium* and *Alloiooccus* were positively correlated with *Moraxella* throughout, with correlation strength increasing significantly over time (Figure 4A; Fisher's r to Z transformation comparing *Moraxella*-*Corynebacterium* and *Moraxella*-*Alloiooccus* correlations before and after 2 years: $p = 9 \times 10^{-14}$ and $p = 7 \times 10^{-16}$, respectively). *Coryne-*

bacterium and *Alloiooccus* were negatively correlated with the illness-associated *Haemophilus* and *Streptococcus* OTUs in early years, but became positively correlated (*Streptococcus*) or uncorrelated (*Haemophilus*) in later samples (Figures 4A and 4B). We hypothesized that the increasing co-occurrence with *Moraxella* might explain the increasing association of *Alloiooccus* with ARI symptoms in later years. Indeed, adjusting for the abundance of *Moraxella* OTU 4398454 resulted in attenuation of the positive association of *Alloiooccus* with ARI after 2 years, but not the negative association with ARI prior to 2 years; whereas adjusting for the abundance of *Alloiooccus* has no effect on the association of *Moraxella* with ARI (Figure 3B). We interpret this to suggest that the apparent negative association between simple *Alloiooccus*-dominated communities before age 2 is likely due to the absence of pathogen-dominated communities rather than any actual protective effect of *Alloiooccus*. The negative association disappears in later years when bacterial diversity is greater and the presence of *Alloiooccus* is less likely to signal the absence of *Moraxella*, which itself is consistently positively associated with ARI. *Staphylococcus* was positively correlated with the health-associated *Streptococcus* 509773 (SparCC correlation = 0.22, $p = 0.001$) but negatively correlated with the illness-associated group as well as *Corynebacterium* and *Alloiooccus*.

We tested for common human respiratory viruses in all samples from the first three years of life; viruses were frequently detected in ARI samples (83% and 81% among URI and LRI, respectively). Interestingly, the same viruses were also detected among 34% of healthy samples, which had been collected after at least 1 month without ARI symptoms. The presence of virus was significantly associated with illness-associated MPGs (compared with health-associated MPGs) irrespective of symptom status (OR 2.4, $p = 1.1 \times 10^{-6}$ in healthy samples; OR 1.9, $p = 1.0 \times 10^{-3}$ in ARI samples using Fisher's exact test; Figure S5), suggesting either

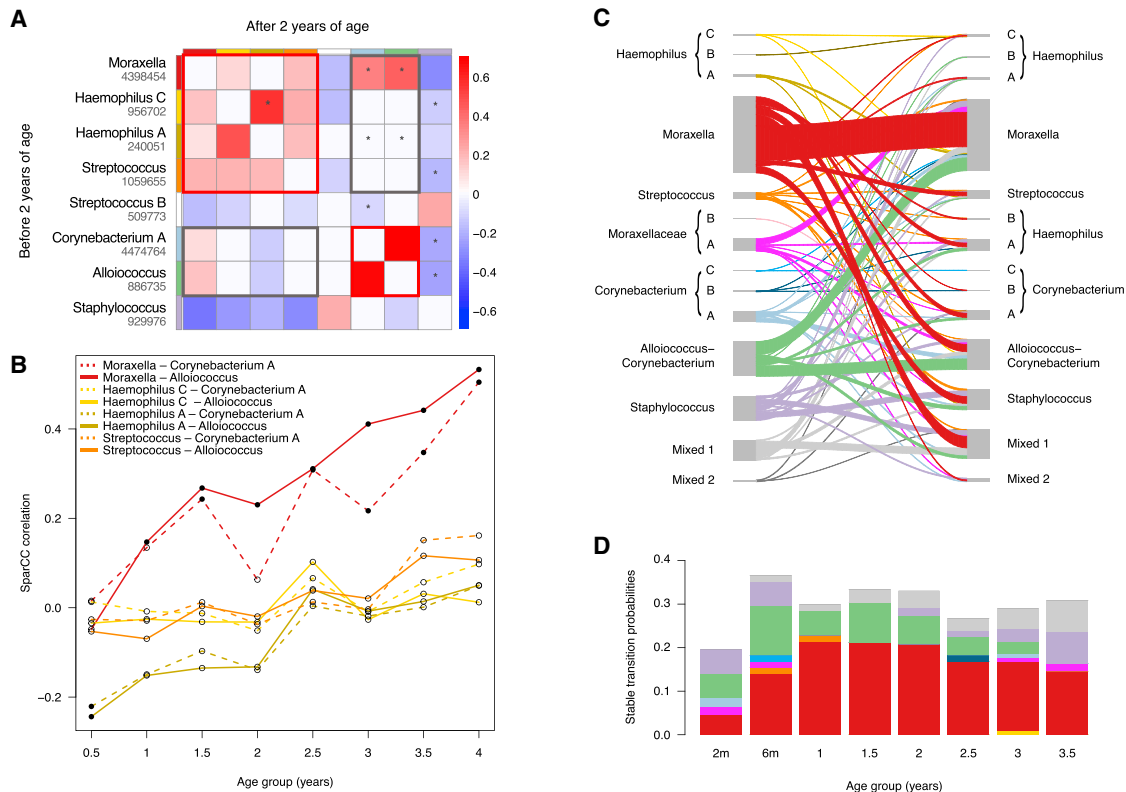


Figure 4. Microbial Interaction Networks and Stability

(A) Pairwise correlations among eight characteristic OTUs, calculated separately for samples collected up to and including 2 years of age (triangle of the heatmap below the diagonal), and samples collected after 2 years of age (triangle of the heatmap above the diagonal). Cell colors indicate correlation coefficients; non-significant correlations ($p > 0.001$) are white. *Bonferroni-corrected $p < 0.05/28$, testing for change in correlation before and after 2 years of age using Fisher's z test.

(B) Correlations between *Alloiooccus* or *Corynebacterium* and *Moraxella* or *Streptococcus* or *Haemophilus* OTUs (bold gray box in A) over half-yearly time periods (filled circles, significant correlations, $p = 0.001$; empty circles, non-significant correlations, $p > 0.001$).

(C) Transitions between microbiome profile groups (MPGs) for consecutive pairs of healthy samples collected from the same individuals 6–12 months apart. OTU key: *Haemophilus*: A = 240051, B = 4469627, C = 956702; *Moraxellaceae*: A = 1057260, B = 854899; *Corynebacterium*: A = 4474764, B = 1049188, C = 4376867.

(D) Proportion of healthy samples collected at each time point, for which the same MPG was detected in the next healthy sample from each individual. Colors indicate the specific MPGs involved, colored as in (C).

See also Figure S6 and Table S4.

mutualism, or synergistic effects on symptomatology, between these specific bacterial communities and common respiratory viruses. However, *Streptococcus*, *Moraxella*, and *Haemophilus* MPGs were also independently associated with ARI symptoms among samples in which no respiratory viruses were detected, or when adjusting for the presence of respiratory viruses or of the specific viruses, RSV or RV (Figures 5A and 5B). This suggests that either these bacteria contribute directly to illness, in the absence of known respiratory viral triggers, which is not unexpected given we predict they are dominated by known respiratory pathogens *S. pneumoniae*, *Moraxella catarrhalis*, and *H. influenzae*; or there is another unknown trigger (e.g., a novel virus) that promotes the overgrowth of these bacteria.

Stability of the Upper Airway Microbiota within Individuals

The NPM is a complex ecosystem that is inherently dynamic as it is continually being shaped by multiple factors, including responses to environmental perturbation and disease status of

the host. We therefore examined the effects of external factors, including ARI and antibiotic exposure, on intra-individual NPM dynamics.

We first considered consecutive healthy samples from each individual, excluding sample pairs collected more than 1 year apart. Overall, the probability of the next consecutive healthy sample sharing the same (non-mixed) MPG as the current sample (i.e., a stable transition) was greater than expected by chance (31% versus 18% for samples collected <6 months apart, binomial test $p = 2.3 \times 10^{-7}$; 23% versus 18% for samples collected 6–12 months apart, $p = 0.011$), indicating some degree of stability of the microbial communities within individuals over time. This stable transition probability was highest for the *Moraxella* (45%) and *Alloiooccus-Corynebacterium* (32%) MPGs, which were the most common states for healthy NPM samples (Figure 4C). Where a sample was assigned to the mixed1 MPG, the probability of the next sample also being designated mixed1 was high (30%). However, the composition of such samples can vary widely, and Bray-Curtis distances between consecutive mixed1

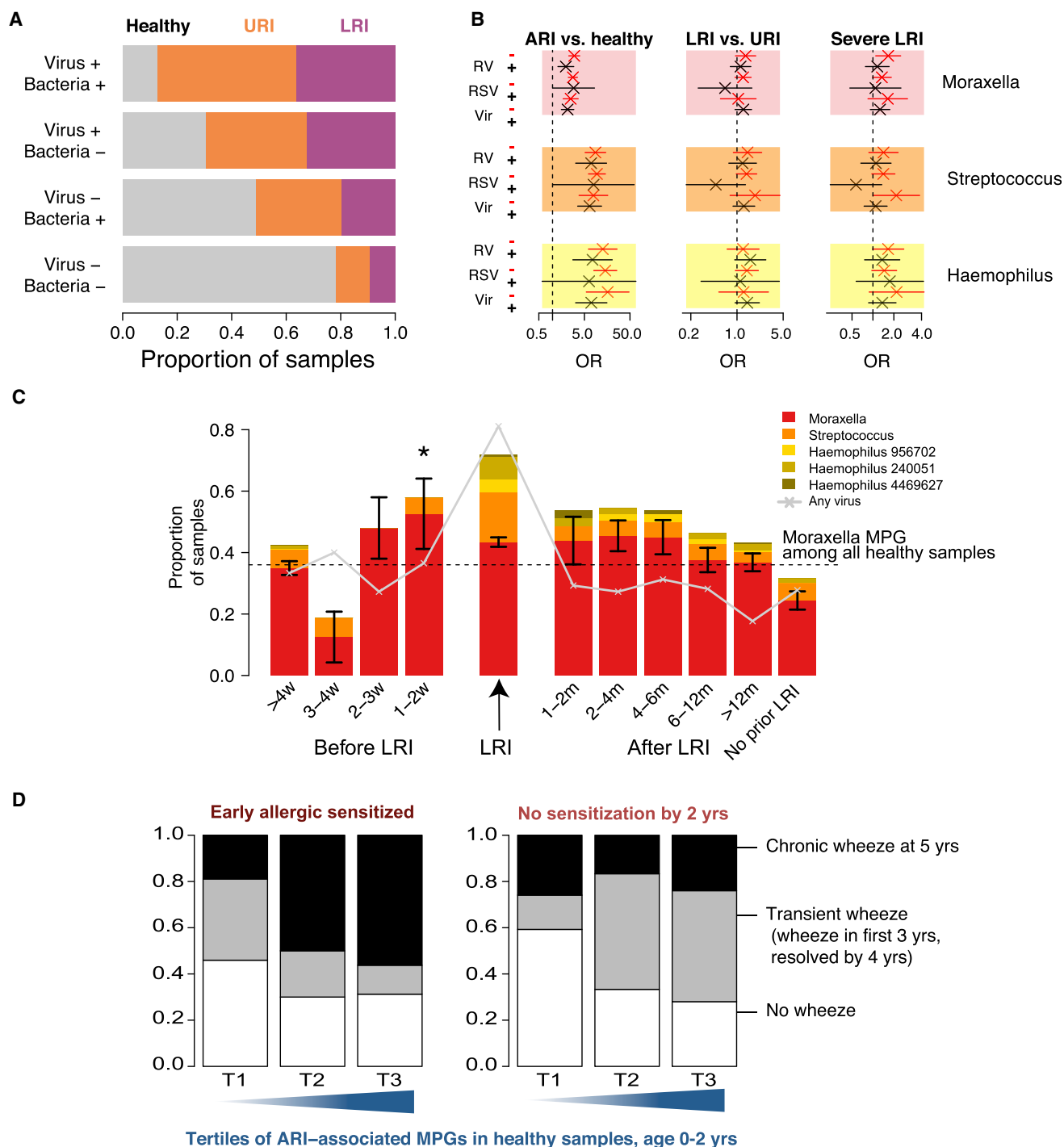


Figure 5. NPM Associations with Symptoms of Acute Respiratory Illness and Wheeze

(A) Frequency of symptoms (URI, upper respiratory illness; LRI, lower respiratory illness) among samples stratified by the presence or absence (+/-) of known respiratory viruses and presence or absence (+/-) of bacterial communities assigned to *Moraxella*, *Streptococcus*, or *Haemophilus* microbiome profile groups (MPGs).

(B) Association of acute respiratory illness (ARI) symptoms with specific MPGs, stratified by the presence or absence (+/-) of common respiratory viruses (RV, rhinovirus; RSV, respiratory syncytial virus; Vir, any virus). Odds ratios (OR) and 95% confidence intervals were estimated using generalized estimating equations with unstructured correlation and robust standard errors, adjusting for age, gender, and season.

(C) Proportion of healthy samples assigned to *Moraxella*, *Streptococcus*, or *Haemophilus* MPGs, stratified by time relative to a recorded LRI episode. SE bars are given for the *Moraxella* MPG. We regressed assignment to *Moraxella* MPG against time to LRI (separate models for each time category versus all other healthy samples) (* $p < 0.05$).

(legend continued on next page)

MPG samples were close to the distances between distinct MPGs (Figure S6), indicating that the majority of consecutive pairs assigned to mixed1 MPG represent significant shifts in NPM composition rather than stable transitions. The probability of a stable transition to the next time point was significantly lower at 2 months of age than at 6-, 12-, 18-, or 24-month time points (Figure 4D; 20% versus 31%; Fisher's exact test, $p = 0.03$), consistent with the observation of a distinct NPM profile at 2 months (Figure 1B). Transition stability declined after 2 years, and an increasing proportion of transitions involved consecutive samples assigned to the mixed1 MPG (Figure 4D), consistent with the observed increase in diversity after age 2 (Figure 2A). The frequency of persistence of the *Staphylococcus* MPG dropped after 6 months and increased again in the fourth year, consistent with prior observations that maternally transferred *Staphylococcus aureus* can be detected in infants, but stable colonization is not established until the pre-school years (Brown et al., 2014; Jimenez-Truque et al., 2012; Schaumburg et al., 2014). Taken together, these results show that the NPM is highly variable in early childhood. Stability of health-associated MPGs was significantly disrupted by the occurrence of LRI during the sampling interval ($p = 0.00042$); however, antibiotic use did not significantly alter the probability of stable transitions ($p = 0.72$; Table S4).

Association of Upper Airway Microbiota with Lower Respiratory Illness and Subsequent Wheeze

LRI was significantly positively associated with *Moraxella*, *Streptococcus*, and *Haemophilus* MPGs, and negatively associated with *Corynebacterium*, *Alloicoccus-Corynebacterium*, and *Staphylococcus* MPGs, especially among samples collected up to 2 years of age (Table S5). This is consistent with our previously reported findings from the first year of life (Teo et al., 2015); but here we had sufficient numbers of pre- and post-LRI asymptomatic samples to also investigate whether LRIs were associated with prior colonization by the illness-associated *Moraxella*, *Streptococcus*, and *Haemophilus* MPGs, and how long these MPGs persisted after an incident LRI. Healthy samples collected 1–2 weeks prior to an LRI were not enriched for viruses (~30% frequency of virus detection, versus 34% across all healthy samples and ~80% during LRI), but were significantly enriched for the *Moraxella* MPG (GEE logistic regression of assignment to *Moraxella* MPG on time to LRI, 1–2 weeks compared with all other healthy samples and adjusted for time post LRI, gender, age, season, recent antibiotics: OR 6.2 [95% confidence interval 1.4–28], $p = 0.017$; further adjusted for viruses: OR 5.9 [1.3–26], $p = 0.019$) (Figure 5C), as well as *Moraxella* abundance (GEE linear regression of log *Moraxella* OTU abundance, $p = 0.025$; further adjusted for viruses: $p = 0.04$) (STAR Methods). There were no significant differences in proportions of *Streptococcus* or *Haemophilus* MPGs nor *Streptococcus* or *Haemophilus* abundance; however, these MPGs were rare (~7%) in healthy samples. We were unable to assess short-term changes in the NPM following LRI, as our criteria for healthy sample collection required the absence of ARI symptoms for at least 4 weeks; how-

ever, the *Moraxella* MPG exhibited declining frequency with increasing time post LRI, and remained enriched until 6 months post LRI (Figure 5C). Interestingly, there was no evidence of a difference in MPG distribution before or after URI (Figure S7).

We have previously shown in this cohort that the risk of chronic wheeze at 5 years of age is significantly associated with the number of LRIs in the first year of life. This was especially the case for the number of febrile LRIs among children with allergic sensitization by age 2 (Kusel et al., 2007, 2012; Teo et al., 2015). Here, we investigated whether presence of the illness-associated *Moraxella*, *Streptococcus*, and *Haemophilus* MPGs during the first four years of life was predictive of LRI intensity during the same period, and/or wheeze at age 5. For each child, we calculated the combined frequency of these MPGs among healthy NPM samples over different time periods (STAR Methods). Among children with early allergic sensitization, frequent ARI-associated MPGs ($\geq 50\%$ of healthy NPM samples) during the first two years of life was significantly positively associated with the number of LRIs experienced in the same period (Table 1). Importantly, among these early-sensitized children, the frequency of illness-associated MPGs in the first two years of life was independently associated with chronic wheeze at 5 years of age (Figure 5D), even after adjusting for LRI frequency and type (Table 2). Notably, among non-sensitized children, the frequency of illness-associated MPGs was not associated with chronic wheeze at 5 years but was significantly positively associated with the transient wheeze phenotype (defined as any wheeze in the first three years of life but no wheeze in the fifth year) (Figure 5D and Table 2). We also note that LRI frequency in years 3–4 was associated with wheeze at age 5 regardless of sensitization status, which we attribute to recent respiratory inflammation being more directly linked to current wheeze (Table 2). There were no significant associations between sensitization status and LRI severity, i.e., the raw frequency or relative proportion of severe (febrile or wheezy) LRIs (Kruskal test, $p > 0.05$ for all time points).

DISCUSSION

This study presents a comprehensive, longitudinal characterization of the upper airway microbiome in a cohort followed from birth to 5 years of age, and its association with episodes of ARI, allergic sensitization, and subsequent wheezing phenotypes. We found the NPM from birth to 5 years of age remains dominated by six common genera (Figure 1) and has yet to converge to an adult-like NPM, which is characterized by much greater alpha diversity, lack of *Moraxella* and *Corynebacterium*, and much lower biomass (Stearns et al., 2015). This is in contrast to the oropharynx (Stearns et al., 2015) or the gut microbiome, which matures to an adult-like state by 3 years of age (Yatsuneneko et al., 2012). The NPM is composed of robust internally homogeneous MPGs, consistent with existing literature pointing to discrete microbial compositions in the nasopharynx during early childhood (Biesbroek et al., 2014; Bisgaard et al., 2007; Bogaert et al., 2011; Bosch et al., 2017; Teo et al., 2015;

(D) Frequency of pre-school wheeze phenotypes (y axis), stratified by frequency of *Moraxella*, *Streptococcus*, or *Haemophilus* MPGs among healthy samples collected from 6 months to 2 years of age (x axis, in tertiles). Data are shown separately for 73 children who were allergic sensitized by 2 years of age, and 64 who were not.

See also Figures S5 and S7.

Table 1. Associations between Proportion of Illness-Associated MPGs in Healthy Samples and LRI Frequency

Outcome	Early Allergic Sensitization		All Other Children	
	MPGs 6m–2y (n = 74)	MPGs 2.5y–4y (n = 83)	MPGs 6m–2y (n = 65)	MPGs 2.5y–4y (n = 65)
# LRI at ages 0 to 1	1.6 (1–2.6), p = 0.043	1.1 (0.83–1.5), p = 0.49	1.5 (0.95–2.3), p = 0.081	1.1 (0.79–1.5), p = 0.57
# LRI at ages 1 to 2	1.5 (1–2.2), p = 0.036	1.1 (0.81–1.5), p = 0.6	1.4 (0.91–2.1), p = 0.12	1.2 (0.81–1.7), p = 0.38
# LRI at ages 2 to 4	1.4 (1–1.9), p = 0.032	1.1 (0.79–1.4), p = 0.72	0.99 (0.79–1.2), p = 0.93	1.1 (0.87–1.3), p = 0.47
# Febrile LRI at ages 0 to 1	2.5 (1–6.3), p = 0.049	1.2 (0.63–2.4), p = 0.53	2.2 (0.77–6.1), p = 0.14	0.84 (0.36–2), p = 0.69
# Febrile LRI at ages 1 to 2	1.8 (0.85–3.6), p = 0.13	0.59 (0.3–1.2), p = 0.13	2.4 (0.65–8.9), p = 0.19	1.8 (0.71–4.6), p = 0.21
# Febrile LRI at ages 2 to 4	1.8 (0.88–3.9), p = 0.11	0.99 (0.5–2), p = 0.98	1.6 (0.74–3.5), p = 0.23	1.4 (0.76–2.5), p = 0.3

m, months; y, years. We modeled the proportion of illness-associated *Moraxella*, *Haemophilus*, and *Streptococcus* MPGs present among healthy samples ($\geq 50\%$ versus $<50\%$) on LRI or febrile LRI frequency using logistic regression. Separate models were fit for different time periods, and for children with and without early allergic sensitization. Values indicate odds ratios (95% confidence intervals) and p values for the association between LRI count and illness-associated MPG frequency $\geq 50\%$ (collected during the period specified in the column header, i.e., 6m–2y or 2.5y–4y).

Tsai et al., 2015). Consistent with previous observations (Biesbroek et al., 2014), we found a constant level of NPM diversity over the first two years of life, followed by a period of increasing diversity, in terms of both number and equitability of OTUs, for at least 3 years (Figures 2A and S3). This increasing diversity coincided with a change in the relationship between the NPM and respiratory disease, whereby negative associations between MPGs and ARI became attenuated (as in the case of *Corynebacterium*) or changed direction to become positively associated with ARI (*Alloicoccus*) (Figure 3A). In the latter case, this appears to be driven by an increasing alliance with *Moraxella* (Figures 3B and 4), which itself was ARI associated. *Moraxella* establishes biofilms that enhance the co-survival of pathogens such as *S. pneumoniae* and *H. influenzae* (Pearson et al., 2006; Perez et al., 2014). It is not yet clear whether the negative associations of certain taxa with ARI denote active protective effects, or simply the lack of pathogenic drivers of symptoms; however, there is some evidence from murine models that pre-exposure to *Corynebacterium* can provide some resistance against RSV infection (Kanmani et al., 2017).

Our longitudinal data show the NPM can be highly dynamic within individuals. However, there was some stability even between samples collected 6 or 12 months apart (Figures 4C and 4D), especially for the MPGs dominated by *Moraxella* or *Alloicoccus* and *Corynebacterium*, which appear to be stable colonizers of the nasopharynx of children. Notably, stability of the *Alloicoccus-Corynebacterium* MPG was significantly reduced by LRI episodes, which are typically associated with an influx and/or overgrowth of *Moraxella*, *Streptococcus*, or *Haemophilus* that can presumably destabilize the bacterial community. This is consistent with a recent study that reported reduced stability of the NPM during infancy among children who experienced more than two ARIs in the first year of life (Bosch et al., 2017). Ultimately, more comprehensive description of natural NPM dynamics, including detailed assessment of resilience to exogenous agents, will require higher-resolution sampling (weekly or daily) and would also benefit from larger cohorts.

Throughout the first five years of life, NPM samples collected during ARIs showed a greater abundance of, and were more commonly dominated by, specific *Streptococcus*, *Moraxella*, and *Haemophilus* OTUs (Figures 1 and 3; Table S2), consistent with expectations regarding common respiratory pathogens *S. pneumoniae*, *M. catarrhalis*, and *H. influenzae* to which these

OTU sequences were most closely related (Table S1). The relative abundances of these OTUs were significantly correlated with one another (Figure 4A); we hypothesize that this is related to the protection provided by the *Moraxella* biofilm (Tan et al., 2007), which can release outer membrane surface proteins that protect other bacteria from complement-dependent killing. Other groups have previously reported reduced upper airway microbial diversity during or prior to ARIs (Frank et al., 2010; Santee et al., 2016; Yi et al., 2014); our data support this, in terms of both enrichment of a small number of community profiles (MPGs) during ARI, and a higher abundance of ARI-associated OTUs and lower alpha diversity within these MPGs compared with that observed in the absence of ARI symptoms (Figures 2B and S3; Tables S2 and S3). We therefore propose that overgrowth of these particular taxa may tip the balance toward respiratory symptomatology, either by direct action as invasive pathogens or via indirect dysregulation of the local immunological milieu. Such dysregulation may increase the likelihood of a primary viral infection of the nasopharyngeal mucosa, or subsequent spread of infection to the lower airways, as suggested in our earlier study on this cohort during infancy (Teo et al., 2015). This is further supported by the increased prevalence of *Moraxella* in asymptomatic samples collected 1–2 weeks before an LRI (Figure 5C). Most LRIs (>80%) had a known respiratory virus present, and this is likely the trigger for acute symptoms. However, the lack of enrichment for viruses, but enrichment for *Moraxella*, in the 1–2 weeks preceding LRI suggests that having the bacteria present when the virus is encountered increases the likelihood of severe respiratory illness. While our study had insufficient power to detect similar effects for *Streptococcus* and *Haemophilus*, due to low colonization frequency in our cohort, there is a large body of evidence accumulating around specific mechanisms of interaction between human respiratory viruses (mainly RV, RSV, and influenza) and *S. pneumoniae*, *H. influenzae*, and *M. catarrhalis*; including both viral promotion of bacterial colonization and outgrowth (for which we see evidence in the form of increased abundance of pathogenic genera in ARIs), and bacterial promotion of viral receptor expression on host cells (Bosch et al., 2017; Brealey et al., 2015). While the present study cannot address specific mechanisms it provides evidence for interactions in both directions, and demonstrates that bacterial colonization influences subsequent ARI throughout infancy and early childhood.

Table 2. Prediction of Subsequent Wheeze Phenotypes Based on Proportion of Illness-Associated MPGs among Healthy Samples during the First Two Years of Life

Data Subset	Model ($Y \sim \text{MPG} + X$)		Predictor = MPG		Predictor = X	
	Y	X	OR (95% CI)	p	OR (95% CI)	p
Early-sensitized children (n = 73)	wheeze at 5y (n = 26)	none	2.5 (1.3–4.6)	0.0054	NA	
		# LRI (year 1)	2.2 (1.1–4.2)	0.018	1.5 (0.94–2.5)	0.085
		# LRI (year 2)	2.3 (1.2–4.3)	0.013	1.3 (0.89–1.8)	0.18
		# LRI (years 3–4)	2 (0.94–4.2)	0.073	2.4 (1.5–3.9)	0.00059
		# febrile LRI (year 1)	2.1 (1.1–4.1)	0.026	2.9 (1.1–7.5)	0.032
	transient wheeze (n = 19)	none	0.5 (0.23–1.1)	0.074	NA	
		# LRI (year 1)	0.44 (0.19–0.99)	0.047	1.4 (0.8–2.3)	0.26
		# LRI (year 2)	0.41 (0.17–0.96)	0.039	1.3 (0.93–1.9)	0.12
		# LRI (year 3–4)	0.54 (0.25–1.2)	0.12	0.86 (0.6–1.2)	0.39
		# febrile LRI (year 1)	0.48 (0.22–1.1)	0.068	1.3 (0.45–3.5)	0.67
All other children (n = 64)	wheeze at 5y (n = 15)	none	0.94 (0.5–1.8)	0.86	NA	
		# LRI (year 1)	0.93 (0.49–1.8)	0.83	1.1 (0.73–1.5)	0.74
		# LRI (year 2)	0.91 (0.46–1.8)	0.78	1.5 (0.99–2.2)	0.059
		# LRI (years 3–4)	1.2 (0.49–3)	0.66	3.8 (1.8–8.3)	0.00062
		# febrile LRI (year 1)	0.94 (0.49–1.8)	0.84	1.2 (0.42–3.2)	0.76
	transient wheeze (n = 22)	none	2.2 (1.2–4.1)	0.014	NA	
		# LRI (year 1)	2.2 (1.1–4.2)	0.022	1.5 (1–2.2)	0.027
		# LRI (year 2)	2.2 (1.2–4.1)	0.014	1.1 (0.75–1.6)	0.62
		# LRI (years 3–4)	2.3 (1.2–4.6)	0.014	0.53 (0.3–0.92)	0.024
		# febrile LRI (year 1)	2.2 (1.1–4.3)	0.018	3.4 (1.2–9.5)	0.018

NA, not applicable; CI, confidence interval. Logistic regression of wheeze phenotype (Y) against tertiles of the proportion of illness-associated *Moraxella*, *Haemophilus*, and *Streptococcus* MPGs (X), adjusting for illness frequency. Separate models were fit for children with and without early allergic sensitization by 2 years of age.

Finally, we found a significant relationship between asymptomatic colonization of the upper airways by certain MPGs in the first two years of life and later wheezing phenotypes, conditional on early allergic sensitization (Figure 5D and Table 2). This builds on the results described in our previous study looking only at the first year of life, where we found that early-life colonization with *Streptococcus* was a risk factor for later childhood wheeze that is exacerbated by early allergic sensitization (Teo et al., 2015). In the present study, we identified that in early-sensitized children, asymptomatic colonization of the upper airways by all illness-associated MPGs (*Streptococcus*, *Haemophilus*, and *Moraxella*) increased the risk of chronic wheeze at 5 years of age, while in children who had not developed early allergic sensitization, it was associated only with transient early wheeze, which resolved by the fourth year of life. Furthermore, in early-sensitized children the frequency of asymptomatic colonization with illness-associated MPGs was also associated with recurrence of LRIs, particularly those accompanied by fever, throughout the first four years of life (Table 1). Notably, however, while frequency of LRI is associated with 5-year chronic wheeze (Kusel et al., 2007; Teo et al., 2015), the effect of bacterial colonization on 5-year wheeze remained after adjusting for LRI (Table 2). It has been suggested that the pathogenic bacterial species *S. pneumoniae*, *H. influenzae*, and *M. catarrhalis* induce local immunoinflammatory responses in the upper airways of neonates, which in the case of *M. catarrhalis* and *H. influenzae* include upregulation of a mix of Th1/Th2/Th17 cytokines (Folsgaard et al.,

2013). However, how these immune responses differ between sensitized and non-sensitized children is incompletely understood. We have suggested, based on previous studies in this and other asthma-risk cohorts (Holt and Sly, 2012), that the increased severity of these episodes in children with allergic sensitization is due in part to interactions between infection-associated type 1 interferon-mediated and allergy-associated Th2-mediated inflammatory pathways, which compromise their capacity to efficiently clear respiratory pathogens, thus worsening ensuing airway inflammation and resultant immunopathology. Conversely, host immune defense mechanisms in those who are non-sensitized are not compromised by these interactions, and they accordingly experience only transient illnesses. This effect may not be confined to bacterial microbiota; others have described causal relationships and synergistic interaction between allergic sensitization and viral infection, particularly rhinovirus (Jackson et al., 2012; Rubner et al., 2017).

In conclusion, this study suggests that the microbiota of the upper airways is an important determinant of the susceptibility, frequency, and severity of ARI in early childhood. In conjunction with early allergic sensitization, the dominating presence of illness-associated MPGs (*Streptococcus*, *Haemophilus*, and *Moraxella*) in the upper airways is a significant risk factor for persistent wheeze in school-age children, which is the hallmark of the asthma phenotype. This observation is of potential importance in relation to early detection and prevention of asthma. In particular, sensitized children in this cohort already showed

elevated levels of allergen-specific immunoglobulin E production from 6 months of age (Holt et al., 2010), suggesting that a high-risk group could be identified in infancy. Airway microbiome monitoring and potential modification might be beneficial for this high-risk group in reducing the risk of LRI, the repeated occurrence of which is closely linked to asthma development.

STAR★METHODS

Detailed methods are provided in the online version of this paper and include the following:

- [KEY RESOURCES TABLE](#)
- [CONTACT FOR REAGENT AND RESOURCE SHARING](#)
- [EXPERIMENTAL MODEL AND SUBJECT DETAILS](#)
 - [Sample and Data Collection](#)
- [METHOD DETAILS](#)
 - [Bacterial 16S Profiling](#)
 - [Virus Detection](#)
- [QUANTIFICATION AND STATISTICAL ANALYSIS](#)
 - [Clustering into Microbiome Profile Groups](#)
 - [Association of Bacterial OTUs with Symptoms of Acute Respiratory Illness](#)
 - [Correlations between Bacterial OTUs](#)
 - [Within-Individual Dynamics](#)
 - [Statistical Methods](#)
 - [Definition of Variables Used in Statistical Analyses](#)
 - [OTU and Microbiome Profile Group \(MPG\) Distributions and Associated Predicted Species](#)
- [DATA AND SOFTWARE AVAILABILITY](#)

SUPPLEMENTAL INFORMATION

Supplemental Information includes seven figures and five tables and can be found with this article online at <https://doi.org/10.1016/j.chom.2018.08.005>.

ACKNOWLEDGMENTS

Supported in part by the Victorian Government's Operational Infrastructure Support Program. This work was supported by the NHMRC of Australia (project grant no. 1049539 to M.I. and K.E.H., Fellowships 1061409 to K.E.H., and 1061435 to M.I.). K.E.H. is supported by a Senior Medical Research Fellowship from the Viertel Foundation of Australia.

AUTHOR CONTRIBUTIONS

M.I. and K.E.H. conceived and directed the project, interpreted the results, and wrote the manuscript. P.G.H. and P.D.S. established the CAS cohort, directed the project, interpreted the results, and wrote the manuscript. S.M.T. and H.H.F.T. performed the bioinformatics and statistical analyses, interpreted the results, and wrote the manuscript. D.M., L.M.J., and K.P. did the DNA extractions, amplification, and amplicon sequencing for the bacterial 16S profiling. S.C.W. performed bioinformatics analysis. B.J.H., M.K., M.S., and N.T. did the sample collection and coordination of databases. Y.A.B., K.G., R.F.L., S.L.J., and J.E.G. did the viral profiling. All authors read and approved the manuscript.

DECLARATION OF INTERESTS

The authors declare no competing interests.

Received: January 12, 2018
 Revised: June 8, 2018
 Accepted: July 13, 2018
 Published: September 12, 2018

REFERENCES

- Australian Commission on Safety and Quality in Health Care. (2017). AURA 2017: Second Australian Report on Antimicrobial Use and Resistance in Human Health (ACSQHC).
- Benjamini, Y., and Hochberg, Y. (1995). Controlling the false discovery rate: a practical and powerful approach to multiple testing. *J. R. Stat. Soc.* *57*, 289–300.
- Biesbroek, G., Tsivtsivadze, E., Sanders, E.A., Montijn, R., Veenhoven, R.H., Keijser, B.J., and Bogaert, D. (2014). Early respiratory microbiota composition determines bacterial succession patterns and respiratory health in children. *Am. J. Respir. Crit. Care Med.* *190*, 1283–1292.
- Bisgaard, H., Hermansen, M.N., Buchvald, F., Loland, L., Halkjaer, L.B., Bonnelykke, K., Brasholt, M., Heltberg, A., Vissing, N.H., Thorsen, S.V., et al. (2007). Childhood asthma after bacterial colonization of the airway in neonates. *N. Engl. J. Med.* *357*, 1487–1495.
- Bochkov, Y.A., Grindle, K., Vang, F., Evans, M.D., and Gern, J.E. (2014). Improved molecular typing assay for rhinovirus species A, B, and C. *J. Clin. Microbiol.* *52*, 2461–2471.
- Bogaert, D., Keijser, B., Huse, S., Rossen, J., Veenhoven, R., van Gils, E., Bruin, J., Montijn, R., Bonten, M., and Sanders, E. (2011). Variability and diversity of nasopharyngeal microbiota in children: a metagenomic analysis. *PLoS One* *6*, e17035.
- Bosch, A.A., de Steenhuijsen Pijters, W.A., van Houten, M.A., Chu, M., Biesbroek, G., Kool, J., Pernet, P., de Groot, P.C.M., Eijkemans, M.J.C., Keijser, B.J.F., et al. (2017). Maturation of the infant respiratory microbiota, environmental drivers and health consequences: a prospective cohort study. *Am. J. Respir. Crit. Care Med.* *196*, 1582–1590.
- Brealey, J.C., Sly, P.D., Young, P.R., and Chappell, K.J. (2015). Viral bacterial co-infection of the respiratory tract during early childhood. *FEMS Microbiol. Lett.* *362*, <https://doi.org/10.1093/femsle/fnv062>.
- Brown, A.F., Leech, J.M., Rogers, T.R., and McLoughlin, R.M. (2014). *Staphylococcus aureus* colonization: modulation of host immune response and impact on human vaccine design. *Front. Immunol.* *4*, 507.
- Camacho, C., Coulouris, G., Avagyan, V., Ma, N., Papadopoulos, J., Bealer, K., and Madden, T.L. (2009). BLAST+: architecture and applications. *BMC Bioinformatics* *10*, 421.
- Caporaso, J.G., Lauber, C.L., Walters, W.A., Berg-Lyons, D., Huntley, J., Fierer, N., Owens, S.M., Betley, J., Fraser, L., Bauer, M., et al. (2012). Ultra-high-throughput microbial community analysis on the Illumina HiSeq and MiSeq platforms. *ISME J.* *6*, 1621–1624.
- Durack, J., Boushey, H.A., and Lynch, S.V. (2016). Airway microbiota and the implications of dysbiosis in asthma. *Curr. Allergy Asthma Rep.* *16*, 52.
- Edgar, R.C. (2004). MUSCLE: multiple sequence alignment with high accuracy and high throughput. *Nucleic Acids Res.* *32*, 1792–1797.
- Ferkol, T., and Schraufnagel, D. (2014). The global burden of respiratory disease. *Ann. Am. Thorac. Soc.* *11*, 404–406.
- Folsgaard, N.V., Schjorring, S., Chawes, B.L., Rasmussen, M.A., Krogfelt, K.A., Brix, S., and Bisgaard, H. (2013). Pathogenic bacteria colonizing the airways in asymptomatic neonates stimulates topical inflammatory mediator release. *Am. J. Respir. Crit. Care Med.* *187*, 589–595.
- Frank, D.N., Feazel, L.M., Bessesen, M.T., Price, C.S., Janoff, E.N., and Pace, N.R. (2010). The human nasal microbiota and *Staphylococcus aureus* carriage. *PLoS One* *5*, e10598.
- Friedman, J., and Alm, E.J. (2012). Inferring correlation networks from genomic survey data. *PLoS Comput. Biol.* *8*, e1002687.
- Galtier, N., Gouy, M., and Gautier, C. (1996). SEAVIEW and PHYLO_WIN: two graphic tools for sequence alignment and molecular phylogeny. *Comput. Appl. Biosci.* *12*, 543–548.
- Guindon, S., Dufayard, J.F., Lefort, V., Anisimova, M., Hordijk, W., and Gascuel, O. (2010). New algorithms and methods to estimate maximum-likelihood phylogenies: assessing the performance of PhyML 3.0. *Syst. Biol.* *59*, 307–321.

- Harimaya, A., Takada, R., Hendolin, P.H., Fujii, N., Ylikoski, J., and Himi, T. (2006). High incidence of *Alloicoccus otitidis* in children with otitis media, despite treatment with antibiotics. *J. Clin. Microbiol.* **44**, 946–949.
- Holt, P.G., and Sly, P.D. (2012). Viral infections and atopy in asthma pathogenesis: new rationales for asthma prevention and treatment. *Nat. Med.* **18**, 726–735.
- Holt, P.G., Rowe, J., Kusel, M., Parsons, F., Hollams, E.M., Bosco, A., McKenna, K., Subrata, L., de Klerk, N., Serralha, M., et al. (2010). Toward improved prediction of risk for atopy and asthma among preschoolers: a prospective cohort study. *J. Allergy Clin. Immunol.* **125**, 653–659, 659.e1–659.e7.
- Jackson, D.J., Evans, M.D., Gangnon, R.E., Tisler, C.J., Pappas, T.E., Lee, W.M., Gern, J.E., and Lemanske, R.F., Jr. (2012). Evidence for a causal relationship between allergic sensitization and rhinovirus wheezing in early life. *Am. J. Respir. Crit. Care Med.* **185**, 281–285.
- Jimenez-Truque, N., Tedeschi, S., Saye, E.J., McKenna, B.D., Langdon, W., Wright, J.P., Alsentzer, A., Arnold, S., Saville, B.R., Wang, W., et al. (2012). Relationship between maternal and neonatal *Staphylococcus aureus* colonization. *Pediatrics* **129**, e1252–e1259.
- Kanmani, P., Clua, P., Vizoso-Pinto, M.G., Rodriguez, C., Alvarez, S., Melnikov, V., Takahashi, H., Kitazawa, H., and Villena, J. (2017). Respiratory commensal bacteria *Corynebacterium pseudodiphtheriticum* improves resistance of infant mice to respiratory syncytial virus and Streptococcus pneumoniae superinfection. *Front. Microbiol.* **8**, 1613.
- Kusel, M.M., de Klerk, N.H., Holt, P.G., Keadze, T., Johnston, S.L., and Sly, P.D. (2006). Role of respiratory viruses in acute upper and lower respiratory tract illness in the first year of life: a birth cohort study. *Pediatr. Infect. Dis. J.* **25**, 680–686.
- Kusel, M.M., de Klerk, N.H., Keadze, T., Vohma, V., Holt, P.G., Johnston, S.L., and Sly, P.D. (2007). Early-life respiratory viral infections, atopic sensitization, and risk of subsequent development of persistent asthma. *J. Allergy Clin. Immunol.* **119**, 1105–1110.
- Kusel, M.M., de Klerk, N., Holt, P.G., and Sly, P.D. (2008). Antibiotic use in the first year of life and risk of atopic disease in early childhood. *Clin. Exp. Allergy* **38**, 1921–1928.
- Kusel, M.M., Keadze, T., Johnston, S.L., Holt, P.G., and Sly, P.D. (2012). Febrile respiratory illnesses in infancy and atopy are risk factors for persistent asthma and wheeze. *Eur. Respir. J.* **39**, 876–882.
- Langille, M.G., Zaneveld, J., Caporaso, J.G., McDonald, D., Knights, D., Reyes, J.A., Clemente, J.C., Burkpile, D.E., Vega Thurber, R.L., Knight, R., et al. (2013). Predictive functional profiling of microbial communities using 16S rRNA marker gene sequences. *Nat. Biotechnol.* **31**, 814–821.
- Magoc, T., and Salzberg, S.L. (2011). FLASH: fast length adjustment of short reads to improve genome assemblies. *Bioinformatics* **27**, 2957–2963.
- Man, W.H., de Steenhuijsen Piters, W.A., and Bogaert, D. (2017). The microbiota of the respiratory tract: gatekeeper to respiratory health. *Nat. Rev. Microbiol.* **15**, 259–270.
- Ngo, C.C., Massa, H.M., Thornton, R.B., and Cripps, A.W. (2016). Predominant bacteria detected from the middle ear fluid of children experiencing otitis media: a systematic review. *PLoS One* **11**, e0150949.
- Oksanen, J., Blanchet, F.G., Friendly, M., Kindt, R., Legendre, P., McGlenn, D., Minchin, P.R., O'Hara, R.B., Simpson, G.L., Solymos, P., Stevens, M.H.H., Szocs, E., and Wagner, H. (2018). vegan: Community Ecology Package. R package version 2.5-2. <https://CRAN.R-project.org/package=vegan>.
- Paulson, J.N., Stine, O.C., Bravo, H.C., and Pop, M. (2013). Differential abundance analysis for microbial marker-gene surveys. *Nat. Methods* **10**, 1200–1202.
- Paulson, J.N., Talukder, H., and Bravo, H.C. (2017). Longitudinal differential abundance analysis of microbial marker-gene surveys using smoothing splines. *bioRxiv*. <https://doi.org/10.1101/099457>.
- Pearson, M.M., Laurence, C.A., Guinn, S.E., and Hansen, E.J. (2006). Biofilm formation by *Moraxella catarrhalis* in vitro: roles of the UspA1 adhesin and the Hag hemagglutinin. *Infect. Immun.* **74**, 1588–1596.
- Perez, A.C., Pang, B., King, L.B., Tan, L., Murrah, K.A., Reimche, J.L., Wren, J.T., Richardson, S.H., Ghandi, U., and Swords, W.E. (2014). Residence of *Streptococcus pneumoniae* and *Moraxella catarrhalis* within polymicrobial biofilm promotes antibiotic resistance and bacterial persistence in vivo. *Pathog. Dis.* **70**, 280–288.
- Phipson, B., and Smyth, G.K. (2010). Permutation P-values should never be zero: calculating exact P-values when permutations are randomly drawn. *Stat. Appl. Genet. Mol. Biol.* **9**, Article39.
- R Core Team. (2018). R: A Language and Environment for Statistical Computing (R Foundation for Statistical Computing). <https://www.R-project.org/>.
- Rubner, F.J., Jackson, D.J., Evans, M.D., Gangnon, R.E., Tisler, C.J., Pappas, T.E., Gern, J.E., and Lemanske, R.F., Jr. (2017). Early life rhinovirus wheezing, allergic sensitization, and asthma risk at adolescence. *J. Allergy Clin. Immunol.* **139**, 501–507.
- Santee, C.A., Nagalingam, N.A., Faruqi, A.A., DeMuri, G.P., Gern, J.E., Wald, E.R., and Lynch, S.V. (2016). Nasopharyngeal microbiota composition of children is related to the frequency of upper respiratory infection and acute sinusitis. *Microbiome* **4**, 34.
- Schaumburg, F., Alabi, A.S., Mombo-Ngoma, G., Kaba, H., Zoleko, R.M., Diop, D.A., Mackanga, J.R., Basra, A., Gonzalez, R., Menendez, C., et al. (2014). Transmission of *Staphylococcus aureus* between mothers and infants in an African setting. *Clin. Microbiol. Infect.* **20**, O390–O396.
- Stearns, J.C., Davidson, C.J., McKeon, S., Whelan, F.J., Fontes, M.E., Schryvers, A.B., Bowdish, D.M., Kellner, J.D., and Surette, M.G. (2015). Culture and molecular-based profiles show shifts in bacterial communities of the upper respiratory tract that occur with age. *ISME J.* **9**, 1246–1259.
- de Steenhuijsen Piters, W.A., Sanders, E.A., and Bogaert, D. (2015). The role of the local microbial ecosystem in respiratory health and disease. *Philos. Trans. R. Soc. Lond. B Biol. Sci.* **370**, <https://doi.org/10.1098/rstb.2014.0294>.
- Tan, T.T., Morgelin, M., Forsgren, A., and Riesbeck, K. (2007). *Haemophilus influenzae* survival during complement-mediated attacks is promoted by *Moraxella catarrhalis* outer membrane vesicles. *J. Infect. Dis.* **195**, 1661–1670.
- Tano, K., von Essen, R., Eriksson, P.O., and Sjøstedt, A. (2008). *Alloicoccus otitidis*—otitis media pathogen or normal bacterial flora? *APMIS* **116**, 785–790.
- Teo, S.M., Mok, D., Pham, K., Kusel, M., Serralha, M., Troy, N., Holt, B.J., Hales, B.J., Walker, M.L., Hollams, E., et al. (2015). The infant nasopharyngeal microbiome impacts severity of lower respiratory infection and risk of asthma development. *Cell Host Microbe* **17**, 704–715.
- Tsai, M.H., Huang, S.H., Chen, C.L., Chiu, C.Y., Hua, M.C., Liao, S.L., Yao, T.C., Lai, S.H., Yeh, K.W., Wang, M.P., et al. (2015). Pathogenic bacterial nasopharyngeal colonization and its impact on respiratory diseases in the first year of life: the PATCH Birth Cohort Study. *Pediatr. Infect. Dis. J.* **34**, 652–658.
- Vandamme, P., Gillis, M., Vancanneyt, M., Hoste, B., Kersters, K., and Falsen, E. (1993). *Moraxella lincolni* sp. nov., isolated from the human respiratory tract, and reevaluation of the taxonomic position of *Moraxella osloensis*. *Int. J. Syst. Bacteriol.* **43**, 474–481.
- Vissers, M., de Groot, R., and Ferwerda, G. (2014). Severe viral respiratory infections: are bugs bugging? *Mucosal Immunol.* **7**, 227–238.
- Watts, S.C., Ritchie, S.C., Inouye, M., and Holt, K.E. (2018). FastSpar: rapid and scalable correlation estimation for compositional data. *bioRxiv*. <https://doi.org/10.1101/222190>.
- Yatsunenkov, T., Rey, F.E., Manary, M.J., Trehan, I., Dominguez-Bello, M.G., Contreras, M., Magris, M., Hidalgo, G., Baldassano, R.N., Anokhin, A.P., et al. (2012). Human gut microbiome viewed across age and geography. *Nature* **486**, 222–227.
- Yi, H., Yong, D., Lee, K., Cho, Y.J., and Chun, J. (2014). Profiling bacterial community in upper respiratory tracts. *BMC Infect. Dis.* **14**, 583.
- Zar, H.J., and Ferkol, T.W. (2014). The global burden of respiratory disease—impact on child health. *Pediatr. Pulmonol.* **49**, 430–434.

STAR★METHODS

KEY RESOURCES TABLE

REAGENT or RESOURCE	SOURCE	IDENTIFIER
Biological Samples		
Paediatric nasopharyngeal samples	Private clinics in Perth, Western Australia	N/A
Critical Commercial Assays		
Illumina MiSeq System	Illumina	RRID: SCR_016379
Deposited Data		
Raw sequence data from 16S profiling	This study	SRP056779
Oligonucleotides		
5'-AATGATACGGCGACCACCGAGATCTACACTA TGGTAATTGTGTGCCAGC MGCCGCGGTAA-3'	515F 16S V4 forward primer	(Caporaso et al., 2012)
5'-CAAGCAGAAGACGGCATACGAGATNNNNNNNNNN NNAGTCAGTCAGCCGGACTACHVGGGTWTCTAAT-3'	806R 16S V4 reverse primer	(Caporaso et al., 2012)
Software and Algorithms		
Blast+	(Camacho et al., 2009)	https://blast.ncbi.nlm.nih.gov/Blast.cgi
fastspar	(Watts et al., 2018)	https://github.com/scwatts/fastspar
metagenomeSeq	(Paulson et al., 2013)	https://github.com/HCBravoLab/metagenomeSeq
Picrust v1.0	(Langille et al., 2013)	https://picrust.github.io/picrust/
QIIME Version 1.7	(Caporaso et al., 2012)	qiime.org
Seaview v4.6.2	(Galtier et al., 1996)	http://doua.prabi.fr/software/seaview
SparCC	(Friedman and Alm, 2012)	https://bitbucket.org/yonatanf/sparcc
The R project for statistical computing	(R Core Team, 2018)	https://www.r-project.org

CONTACT FOR REAGENT AND RESOURCE SHARING

Further information and requests for resources and reagents should be directed to and will be fulfilled by the Lead Contact Michael Inouye (minouye@baker.edu.au).

EXPERIMENTAL MODEL AND SUBJECT DETAILS

Sample and Data Collection

This study is part of the Childhood Asthma Study (CAS) – a prospective community-based cohort of 244 children (57% male) at high risk of allergic sensitization (at least one parent with a doctor diagnosed history of asthma, hay fever or eczema) who were followed prenatally until five years of age with the goal of identifying risk factors for allergic diseases, as previously described (Kusel et al., 2006, 2007, 2012; Teo et al., 2015). Children were recruited between 1996 and 1998, before the introduction of the pneumococcal vaccine in Western Australia in 2005. Healthy nasopharyngeal (NP) samples were collected at planned half-yearly visits (first sample from about 2 months of age, subsequently at 6 months, 1 year, and so on), in the absence of any symptoms of acute respiratory illness (ARI) for at least 4 weeks. In addition, parents were to contact a study clinician at the onset of any ARI symptoms, at which point a study nurse visited the family within 48 hours to collect a NP sample from the child and interview the parents on the symptoms and medications used in relation to the illness. ARIs were classified as a lower respiratory illness (LRI) if accompanied by wheeze or rattly chest; or an upper respiratory illness (URI) otherwise. A total of 1943 healthy samples, 2579 URI samples, and 1056 LRI NP samples were collected and divided into aliquots that were cryofrozen for later analysis. Healthy samples that did not fulfil the criterion of >4 weeks after an illness episode were excluded. Parents kept a daily record of any medication used, from which antibiotic exposure information was extracted, and completed yearly questionnaires during face-to-face interviews. Blood samples were collected from each child at 6 months, 1, 2, 3, 4 and 5 years of age, and positive sensitization status at each timepoint was defined as serum IgE levels > 0.35 kU/L to house dust mite, cat epithelium and dander, peanut, foodmix, couch grass, rye grass, mould mix, or infant phadiatop (details of which were described in (Holt et al., 2010)). All models included gender as a covariate.

The study design is a large prospective birth cohort, the gold standard for observational research. There were no interventions thus randomization and blinding were not relevant. Individuals were representative of the local population (Perth, Australia). Replication of this study is not currently feasible as this would require a separate prospective birth cohort with similar environment, sampling, sequencing, clinical follow-up, etc. Future studies are anticipated to address this.

Approval for the study was obtained from the ethics committee of King Edward Memorial and Princess Margaret Hospitals in Western Australia. Fully informed written consent was obtained from the parents for the use of stored samples for research projects.

METHOD DETAILS

Bacterial 16S Profiling

One aliquot from each of 1331 healthy, 996 URI and 1055 LRI samples were prepared for bacterial 16S rRNA amplicon sequencing. Total DNA was extracted using a method combining homogenization and chemical lysis of cells. Extractions were performed in biosafety cabinets that were UV-sterilised, including all plastic-ware, for 30 min prior to the procedure. The samples were thawed from -80°C storage, transferred into 1.5 mL sterile screw-capped tubes and briefly micro-centrifuged. The saline storage buffer was removed and pellets were resuspended in 400 µL of lysis solution supplied with the Wizard SV Genomic DNA System (Promega, Victoria, Australia). Samples were mixed vigorously by pipetting and then transferred into a labelled Lysing Matrix B tube (MP Bio-medicals, New South Wales, Australia). Suspensions were homogenized using a FastPrep-24 homogenizer for 40 s at 6.5 m/s. Following micro-centrifugation, homogenates were transferred into a 1.5 mL screw-capped tube. A further 200 µL of lysis solution was added into each lysing matrix tube and vortexed to wash off any residual homogenate, then transferred to the respective homogenate tube to retain the original lysis volume. Homogenates were then treated with nuclei lysis buffer/RNase A and DNA extraction was carried out using the Wizard SV Genomic DNA System as per manufacturer's instructions. Purified DNA was eluted in 100 µL of pre-warmed sterile low 1 X TE (Fisher Biotec, WA, Australia), aliquoted and stored at -80°C.

Amplicons were prepared for MiSeq sequencing using primers (prepared by Integrated DNA Technologies, Iowa, USA) spanning the V4 region of the 16S rRNA gene and containing barcoded reverse primers as published by Caporaso et al. (Caporaso et al., 2012). The forward universal primer included the 5' Illumina adapter sequence, forward primer pad, linker and the 515F 16S rRNA sequence: 5'-AATGATACGGCGACCACCGAGATCTACACTATGGTAATTGTGTGCCAGC MGCCGCGGTAA-3'. The reverse primer included the 3' Illumina adapter sequence, a 12-mer Golay barcode (denoted as N), reverse primer pad, linker and the 806R 16S rRNA sequence: 5'-CAAGCAGAAGACGGCATACGAGATNNNNNNNNNNNAGTCAGTCAGCCGGACTACHVGGGTWTCTAAT-3'. All laboratory equipment used was wiped with DNA Away (MBP, Mexico) before conducting each PCR procedure. Master mixes were prepared in a UV-treated PCR chamber before they were dispensed into 96-well plates using a Multiprobe II liquid handling system (Perkin Elmer, Victoria, Australia), followed by addition of samples and controls using the robot. Amplification of each sample was performed in quadruplicate to obtain enough amplicon for sequencing. To each plate, a positive control (gDNA from *S. enterica* strain LT2, a bacterium not normally associated with the respiratory system (ATCC#700720D-5, USA)) and water and TE negative controls (obtained from each extraction procedure) were included and assessed for amplification by agarose gel electrophoresis. All controls were as expected: *S. enterica* controls were positive and the water and TE negative controls were negative. Positive control samples were not analysed further, while the negative controls were prepared for sequencing in the same way as samples.

Due to the high throughput nature of this study, we did not quantify and normalize sample DNA that was added into each PCR reaction, rather a fixed volume (4 µL) of DNA template was used per well. Amplification was conducted on a GeneAmp 9700 PCR System (Perkin Elmer) using the following conditions: an initial 94°C denaturation step for 2 min, followed by 30 cycles of 94°C denaturation for 30 s, 58°C annealing for 30 s and 72°C extension for 1 min.

Quadruplicate sample amplicons were combined into a single well on the PCR reaction plate, then transferred to a fresh round-bottom polystyrene plate where they were purified using Agencourt AMPure XP beads as directed by the manufacturer, with slight modifications (Beckman Coulter, USA). Purified amplicons were eluted in 25 µL sterile low 1 X TE buffer (Fisher Biotec). Quantitation of amplicon was performed using the Quant-iT PicoGreen dsDNA quantitation kit (Life Technologies, Victoria, Australia) and fluorescence was determined on a Wallac Victor³ Multilabel counter (Perkin Elmer). PCR samples were equalized to 2 nM concentration (a neat aliquot was used where a sample fell below this concentration) and pools of 48, 60 or 96 barcoded samples were generated and sent for sequencing.

Primer adaptors were removed from library pools using a 0.8x ratio of Agencourt AMPure XP beads (Beckman Coulter, USA). Library quantitation was determined by the high sensitivity Qubit kit (Life Technologies, USA) whilst library quality and average size distribution was assessed by the Bioanalyser (Agilent Technologies, USA) high sensitivity kit. Library pools were diluted to 2nM followed by NaOH denaturation as per manufacturer's instructions (Illumina Inc., USA). Sequencing primers read 1: 5'-TATGG TAATTGTGTGCCAGC MGCCGCGGTAA -3', read 2: 5'-AGTCAGTCAGCCGGACTACHVGGGTWTCTAAT-3' and index: 5'-ATTAGA WACCCBDGTAGTCCGGCTGACTGACT-3' (Sigma, Australia) were spiked into the MiSeq Cartridge at a final concentration of 0.5µM. Denatured libraries were loaded at 6.5pM with a 5% PhiX spike for diversity and sequencing control, onto a v2 300 cycle cartridge for sequencing on the Illumina MiSeq.

Paired end reads were merged using Flash version 1.2.7 (Magoc and Salzberg, 2011) with read length 151 base pairs (bp) and expected fragment length 253 bp. The merged reads were quality filtered as follows: ≤ 3 low-quality bp (Phred quality score < 3) allowed before truncating a read, ≥ 189 consecutive high-quality bp, sequences with any N characters were discarded. Reads were clustered into operational taxonomic units (OTUs) using the closed reference OTU picking method in QIIME v1.7 using the Greengenes 99%

reference database version 13_05. Mean of 1% of reads per sample had no match to the Greengenes database and were excluded from further analysis (except for alpha diversity calculations, as described below). Negative control samples had a median of >1500 (taxonomy-assigned) reads (interquartile range 900 – 2300), while NP samples had a median of >147K reads (IQR 45K – 230K). We therefore removed 142 NP samples with <3000 taxonomy-assigned reads. A total of 3014 samples were left for further analysis, including 1018 healthy samples (median 5 samples per child, IQR 3-6), 964 samples from upper respiratory illnesses (URIs; median 4 samples per child, IQR 2-6), and 1,032 samples from lower respiratory illnesses (LRIs; median 4 samples per child, IQR 2-7).

Because entries in the Greengenes database may be identical in the V4 subregion that we sequenced, it is possible for identical read sequences to be assigned to different Greengenes OTUs. We therefore merged counts for OTUs that were identical in the sequenced V4 region (identified by extracting the sequence between the forward and reverse primer sequences), as shown in [Figure S2](#). Read counts were corrected for OTU-specific copy number using Picrust v1.0 ([Langille et al., 2013](#)) using the pre-computed copy number estimates for Greengenes OTUs version 13_05; and relative abundances were calculated by normalising to the total taxonomy-assigned reads for each sample. Phylogenetic analyses were conducted by BLAST ([Camacho et al., 2009](#)) searching the NCBI 16S rRNA database using representative V4 region sequences from the common taxa ([Figure S1B](#)) to identify similar sequences. For each genus, the sequences were aligned using Muscle ([Edgar 2004](#)) and a maximum-likelihood tree constructed using PhyML ([Guindon et al., 2010](#)) and visualized in Seaview ([Galtier et al., 1996](#)) ([Figure S2](#)); these were used to identify the closest known species for each common OTU ([Table S2](#)).

Virus Detection

A second aliquot from 736 healthy, 583 URI and 789 LRI samples from the first three years (72%, 76% and 60% of all healthy, URI and LRI samples, respectively for which we had 16S profiles), were prepared for viral detection via reverse transcriptase polymerase chain reactions (PCR). Target organisms were: human rhinoviruses (RV); other picornaviruses (coxsackie, echo and enteroviruses); coronaviruses 229E and OC43; respiratory syncytial virus (RSV); influenza A and B; parainfluenzaviruses 1-3; adenoviruses and human metapneumovirus (HMPV). Primers, probes and PCR assay conditions have been previously described ([Bochkov et al., 2014](#); [Kusel et al., 2006, 2007](#)).

QUANTIFICATION AND STATISTICAL ANALYSIS

Clustering into Microbiome Profile Groups

Samples were assigned to microbiome profile groups (MPGs) based on hierarchical clustering of OTU relative abundances, using Bray-Curtis dissimilarity as the distance metric and complete linkage (implemented in the R function *hclust*). These analyses included all common OTUs (defined as mean relative abundance >0.1%, present in >20% of samples, and dominating (>50%) at least one sample); aggregated counts of other OTUs from each of the major genera (*Moraxella*, *Streptococcus*, *Haemophilus*, *Alloicoccus*, *Corynebacterium*, *Staphylococcus*) and family Moraxellaceae; and a final group consisting of aggregated counts of all other OTUs (labelled 'rare OTUs'; see rows in [Figure 1](#)). The number of clusters (i.e. unique MPGs) was chosen to maximise the median silhouette value. MPGs were named based on the dominant genus or OTU, as indicated in [Table S1](#). Alpha (within-sample) diversity was assessed using Shannon's diversity index measure, which takes into account both number and relative abundance of the OTUs.

Association of Bacterial OTUs with Symptoms of Acute Respiratory Illness

We normalized the copy-number-corrected OTU read counts using cumulative sum scaling (CSS) ([Paulson et al., 2013](#)). Briefly, for each sample, the OTU counts were divided by the cumulative sum of counts up to the smallest percentile for which sample-specific count distributions were largely invariant (98.9th percentile for our data). We then tested for differential abundance in ARI vs healthy samples, for each of 1,090 OTUs that were present in >10% of samples. A zero inflated Gaussian mixture model was fitted to the log transformed CSS-normalized OTU counts, separately for samples before and after 2 years of age (before 2 years: inclusive of samples at 2-year timepoint; after 2 years: from 2.5-year timepoint), using the R package *metagenomeSeq* ([Paulson et al., 2013](#)). We summarized the results for OTUs with an absolute fold change of >1.5 and FDR adjusted p-value <0.025 in either age strata. We picked eight representative OTUs to more precisely investigate how the associations changed over time, and modelled the longitudinal structure of the data using smoothing splines ANOVA with 100 permutations to assess significance ([Paulson et al., 2017](#)). All models for the ARI vs. healthy association were adjusted for age, season, gender, and any antibiotics within the last 4 weeks.

Correlations between Bacterial OTUs

We inferred correlation networks among the 1,090 common OTUs present in >10% of samples using FastSpar ([Watts et al., 2018](#)), an efficient C++ implementation of the SparCC algorithm, which was designed to deal specifically with compositional data and produces more reliable and robust correlation estimates compared to Pearson or Spearman correlation especially in the case of low diversity samples ([Friedman and Alm, 2012](#)). SparCC uses a log ratio transformation and calculates correlations between OTUs in an iterative manner, under the assumption of a sparse network. Statistical significance of the correlation was assessed using 1000 bootstrap samples with exact p-value calculations based on the *permp* function in R package *statmod* ([Phipson and Smyth, 2010](#)). Correlation networks were generated across all samples, as well as separately for samples before and after 2 years of age, samples within each half yearly time periods, and samples with low abundance (<1%) of *Moraxella* OTU. We assessed differences in correlation before and after two years using the Fisher's r-to-Z transformation (*cocor* R package).

Within-Individual Dynamics

We first explored microbiome changes within each child in terms of transitions from a healthy sample to the next healthy sample half a year or a year later. Transitions which resulted in a MPG change indicated an abrupt shift in the major OTU (termed “unstable transitions”); stable otherwise. We also assessed the transitions using the Bray-Curtis dissimilarity calculated on the CSS-transformed OTU count matrix using the *vegan* R package (Oksanen et al., 2018), which represented subtle changes. Transition stability and distance were assessed for the effects of intervening ARI, LRI and antibiotics using GEE regression (logistic or linear where appropriate), adjusting for the age of first sample and difference in ages between samples.

We then investigated whether we could detect changes in the NPM prior to ARI symptoms, and how long these changes persisted after the illness. We grouped the healthy samples according to how soon after illness occurred (pre-illness: 1-2 weeks, 2-3 week, 3-4 weeks or >4 weeks) and how long after the last illness episode (post-illness: 1-2 months, 2-4 months, 4-6 months, 6-12 months, or >12 months). We used GEE logistic or linear regression to model (i) assignment to specific illness-associated MPGs or (ii) log abundance of specific illness-associated OTUs, against time to ARI/URI/LRI (separately for each pre-illness time category compared to all other healthy samples), and adjusted for time post-illness, gender, age, season, recent antibiotics, and any virus.

Lastly, we examined per child, if the proportion of illness-associated *Moraxella*, *Haemophilus* and *Streptococcus* MPGs in their healthy asymptomatic samples over different time periods (6 months to 2 years, and 2.5 years to 4 years) was associated with LRI frequency and subsequent wheeze phenotypes (wheeze at age 5 years or transient wheeze). Logistic regression was used to model (i) the proportion of illness-associated MPGs (as a binary: $\geq 50\%$ versus $< 50\%$, excluding children with < 2 healthy samples in each corresponding time period) against LRI and febrile LRI frequency in years 1, 2, 3 and 4, (ii) wheeze phenotypes against proportion of illness-associated MPGs (as tertiles), adjusting for LRI frequency. Separate models were fit for children with and without early allergic sensitization by 2 years of age.

Statistical Methods

All statistical analyses were performed using R (R Core Team, 2018) unless otherwise stated. Association analyses that involved multiple samples from the same subject were modelled using generalized estimating equations (GEE) with unstructured correlation and robust standard errors, where possible. In the case of non-convergence due to insufficient sample size, the ordinary logistic regression was used. Potential confounders were included in the model. We used the Benjamini-Hochberg false discovery rate method (FDR) (Benjamini and Hochberg, 1995) or Bonferroni correction where multiple testing p-value adjustments were needed, as stated. All boxplots shown use the Tukey format, in which the bottom and top of the box represents the lower and upper quartiles respectively and the ends of whiskers represents the lowest/highest datum still within 1.5 interquartile range of the lower/upper quartile.

Definition of Variables Used in Statistical Analyses

- Wheeze at age 5: Presence of wheeze in the last 12 months recorded in the 5 year questionnaire.
- Transient wheeze: Any wheeze in the first three years, but no wheeze in the 5th year.
- Early allergic sensitization: Any allergen-specific IgE levels > 0.35 kU/L by two years of age (at any of 6 month, 1 year or 2 years timepoints).
- Season: According to month of collection: spring (September–November), summer (December–February), autumn (March–May) or winter (June–August).
- Recent antibiotics: Any record of antibiotics intake within the last 4 weeks prior to sample collection.

OTU and Microbiome Profile Group (MPG) Distributions and Associated Predicted Species

The *Moraxella* genus was overwhelmingly represented by OTU 4398454 (*M. catarrhalis*) throughout all five years (Figure S1B). The associated *Moraxella* MPG, which was dominated by this OTU, was of relatively low frequency in the 2-month healthy samples (13%), but increased sharply thereafter, stabilizing at an average of 39% from one year of age. In ARI samples, the *Moraxella* MPG followed a similar trend, increasing from 29% at two months of age to $\sim 43\%$ in the later time periods (Figure 1B). In addition, 5% of all samples fell into one of two MPGs dominated by OTUs classified to the *Moraxellaceae* family (either OTU 1057260 or 854899); NCBI blastn searches of these sequences matched closely to *Moraxella lincolnii* (Figure S2). This species had been previously isolated from the human respiratory tract (ages 6 months – adult) (Vandamme et al., 1993), and was also observed in a 16S analysis of NP samples of children aged 6 months to 2 years in a Dutch population (Biesbroek et al., 2014). In our data, these MPGs were negatively associated with ARI (OR 0.7, $p = 0.016$; Table S2).

The *Streptococcus* genus was mostly represented by OTU 1059655 (67% of all *Streptococcus* reads; orange in Figures 1A and S1), whose representative sequence was closest to the *Streptococcus pneumoniae*–*pseudopneumoniae* complex (Figure S2 and Table S1). The presence of this OTU in ARI samples in the first year was correlated with detectable IgG1 antibodies to *S. pneumoniae* pneumococcal surface protein A1, A2, or C at one year of age as previously reported (Teo et al., 2015). Samples dominated by this OTU clustered into a single MPG we labelled “Streptococcus” (orange in Figure 1B), which was rarely observed in two-month samples but common thereafter (from 6 months: mean of 5% and 14% in healthy and ARI samples, respectively). The next most frequently observed *Streptococcus* OTU was 1004451 (15%; green in Figure S1); its V4 sequence is distinguished from 1059655 by a common base substitution (tree in Figure S2), and is close to many commensal *Streptococcus* species (Table S1). Samples assigned to the “other Streptococcus” MPG were often dominated by this OTU (Figure 1A).

The *Haemophilus* genus was represented by two distinct MPGs dominated by OTU 240051 or 956702 (Figure 1A), both of which show best matches with *H. influenzae* and *H. haemolyticus* sequences (which are not distinguishable at the V4 region; see Figure S2). As previously reported, the presence of these OTUs in ARI samples in the first year was correlated with detectable IgG1/IgG4 antibodies to *H. influenzae* P4/P6 surface proteins at one year of age (Teo et al., 2015). These MPGs were infrequent in the healthy samples (2%), but comprised 11% of ARI samples (Figure 1B). The rare *Haemophilus* OTUs were also close to *H. influenzae* and *H. haemolyticus* sequences, with the exception of 4404220, 4053636 and 3605478 which were distant from these but clustered with *H. parainfluenzae* and *H. parahaemolyticus* (Figure S2) and were occasionally detected in healthy samples (Figure S1).

The *Corynebacterium* genus was primarily represented by OTU 4474764, which best matched the commensal oropharyngeal bacterium *C. propinquum* (Figure S2). A distantly related OTU 4376867 (matching the nasal coloniser *C. accolens*) was detected in infancy (16% of *Corynebacterium* reads in the first 6 months) but very rarely thereafter (Figure S1B; all 17 samples assigned to the associated MPG were collected during the first year of life, 15 (88%) of which in the first 6 months, Figure 1B). Samples dominated (>29%) by OTU 4474764 (closest to *C. propinquum* and *C. pseudodiphtheriticum*) clustered into a single MPG we labelled “*Corynebacterium*”, which was frequent in healthy samples in the first 6 months (10–12%), but declined to <7% thereafter (Figure 1B). *Corynebacterium* OTU 4474764 frequently co-occurred with *Alloiococcus* (overwhelmingly represented by the *A. otidis* / *Dolosigranulum pigrum* OTU 886735), in samples belonging to the *Alloiococcus-Corynebacterium* MPG (median 43% *Alloiococcus* OTU 886735 and 32% *Corynebacterium* OTU 4474764).

The *Staphylococcus* genus was mostly represented by OTU 929976, although there were also numerous low-abundance *Staphylococcus* OTUs that co-occurred with this one (Figure 1A). The *Staphylococcus* MPG (median 43% OTU 929976 and 9% other *Staphylococcus* OTUs) was most common at 2 months (36% and 28% in healthy and ARI samples, respectively) but declined to low levels subsequently in ARI samples (0–11%, Figure 1B). *Staphylococcus* species are not well resolved at the 16S V4 region; OTU 929976 is identical to known sequences from *S. aureus* but also other species (Figure S2).

DATA AND SOFTWARE AVAILABILITY

Sequencing data for this study, cleaned for human reads, has been deposited in the NCBI GenBank (accession SRP056779).